16

X-RAY ASTRONOMICAL SPECTROSCOPY

Stephen S. Holt
Laboratory for High Energy Astrophysics
Goddard Space Flight Center
Greenbelt, Maryland 20771

ABSTRACT

The contributions of the Goddard group to the history of X-ray astronomy are numerous and varied. One unique role that the group has continued to play involves the pursuit of techniques for the measurement and interpretation of the X-ray spectra of cosmic sources. The latest development in this story has been the selection of the new X-ray "microcalorimeter" for the AXAF study payload. This technology is likely to revolutionize the study of cosmic X-ray spectra.

1. INTRODUCTION

X-ray astronomy is currently more than 20 years old, as measured from the first unambiguous discovery of extra-solar X-rays [Giacconi et al., 1962]. Experimental research during this first generation may be broadly classified into four main types of measurement: timing, imaging, polarimetry, and spectroscopy. This review is meant to concentrate primarily on the latter, with specific attention paid to the contributions made by the group at GSFC which was created and nurtured by Frank McDonald.

During the first decade of X-ray astronomy, timing measurements represented the most important channel of investigation. Direct measurements of periodic and Doppler-effected periodic variability signaled the very nature of the strong

X-ray emitters in the galaxy as accreting neutron stars in binary systems [cf. Schreier et al., 1972]. The value of timing measurements has not diminished, as new discoveries continue to be made via the timing channel [e.g., "QPOs", or quasi-periodic oscillations, from some bright galactic bulge sources by Van der Klis et al., 1985, using EXOSAT data], and new capabilities continue to be planned (e.g., the Japanese mission ASTRO-C and the Explorer mission XTE).

The advent of substantial X-ray imaging capability with the Einstein Observatory (HEAO-2), launched in 1978, allowed sensitivities for point source and morphological studies sufficient to make imaging an important research tool [Giacconi et al., 1979]. This trend will continue with the cooperative German/U.S. mission ROSAT, and will be considerably expanded with the advent of the major observatory AXAF.

Polarimetry is extremely difficult for X-ray astronomical sources, and only a single space-borne instrument has thus far been attempted. It achieved important confirmatory evidence for the synchrotron nature of the X-ray emission from the Crab nebula [Weisskopf et al., 1978], but that first instrument lacked the sensitivity to measure the required few percent (or better) polarization in much weaker sources necessary to allow polarization to become a more generally useful tool for X-ray astronomical research.

While all four channels offer important and complementary information, spectroscopy has steadily achieved increasing importance as X-ray astronomy has matured. This review will concentrate on the "new" X-ray spectroscopy, i.e., that which has sufficient resolving power to be concerned with measurements of discrete line features rather than just with continua.

2. INSTRUMENTAL CONSIDERATIONS

Virtually all pre-Einstein X-ray spectroscopy was performed with proportional counters, which have a resolving power limited by the nature of the atomic interactions in the counter gas (which follow the primary photoabsorption) to $R = E/\delta E_{FWHM} \sim 3E_{keV}^{-1/2}$. Early attempts by the GSFC group to search for Fe emission with such counters [Holt, Boldt, and Serlemitsos, 1969] led to the development of large multi-wire proportional chambers which were

ultimately rewarded with positive detections of thermal Fe emission from supernova remnants [Serlemitsos et al., 1973] and fluorescent Fe emission from cold material surrounding the ionization source in galactic X-ray binary sources [Serlemitsos et al., 1975].

Gas scintillation counters, which shortcut the atomic interactions subsequent to primary photoionization, are limited to a resolving power which is higher by a factor of two. Such detectors have successfully been flown on the European EXOSAT and Japanese "Tenma" missions.

Even higher resolving powers in photoelectric detectors can be achieved by using semiconductors instead of gas as the detection medium. The most successful such instrument for X-ray astronomy has been the SSS (solid-state spectrometer), a cryogenically cooled silicon chip with resolving power $R \sim 6E_{keV}$ provided by the GSFC group to the Einstein Observatory (HEAO-2). Like other charge collecting proportional devices, Si(Li) can have detection efficiency approaching unity over its entire bandpass simultaneously. Dispersive devices, such as the Einstein FPCS (focal plane crystal spectrometer, with $R \sim 100$) and the OGS (objective grating spectrometer, with $R \sim 30$), have already demonstrated great analytic power with observations of a few of the brighter sources. Such instruments can be designed to have $R > 1000$, but will require very large collecting areas to be generally useful for a large number of sources because of their low effective photon detection efficiencies. Next generation FPCS and OGS systems have been conditionally selected for the initial complement of AXAF instruments.

Similarly selected is a novel new X-ray spectrometer currently under development at GSFC which is capable, in principle, of combining the high efficiency and bandwidth of the photoelectric devices with the high resolving power of the dispersive devices. The "microcalorimeter" consists of a supercooled chip in which an X-ray is photoelectrically detected and its energy is totally thermalized, with the resultant $\sim 10^{-16}$ joules measured via the rise in temperature of the chip. The system is expected to exhibit a resolving power $R > 1000$ for Fe–K lines.

The problem of translating from photons detected in a spectrometer to a source spectrum is not trivial, and it is important to recognize that the interpretation of an observation can depend upon the analysis procedure employed.

The raw data are a convolution of the actual input photon spectrum with the response function of the spectrometer, but their inversion to a derived input spectrum is not unique.

The conventional inversion is a model-dependent procedure that requires the observer to have some a priori knowledge of the actual spectral form, so that it can be characterized by a limited number of adjustable parameters. Typical fitting parameters are amplitude and shape of continuum (e.g., power law index with exponential high energy cutoff), strengths (and possibly energies) of emission lines and photoelectric absorption edges, and low energy photoabsorption by intervening cold matter. Simulated detector count spectra are computed from the assumed spectral forms, and the model parameters are varied to achieve the best fit to the actual detector counts. With this procedure, spectral features blurred by the detector response can be enhanced for display, as illustrated in Figure 1. Its hazard is that unanticipated features are forced to be represented by the assumed parameters so that, for example, an intrinsically broad line might emerge as a doublet if only sharp lines are assumed. If the lines are totally resolved, however, much of this ambiguity disappears.

3. X-RAY SPECTRAL CATEGORIZATION

The variety of X-ray sources present a variety of observational manifestations; in some cases, X-ray spectra provide unique opportunities to gain crucial insight into the nature of sources.

Since line emission ceases to be the dominant cooling mechanism of astrophysical plasmas for temperatures exceeding $\sim$ 1 keV, X-ray spectra are primarily characterized by their continua. The simplest (at least spectrally) of these are the featureless power laws produced by the interaction of power law distributions of cosmic ray electrons with ambient magnetic fields. The Crab nebula, for example, is the archetype of such a pure synchrotron source, in which we observe the single interaction of astrophysical particles and fields.

Almost as simple, in the sense that it is also a single-parameter continuum, is the blackbody spectrum which characterizes the other extreme, i.e., the

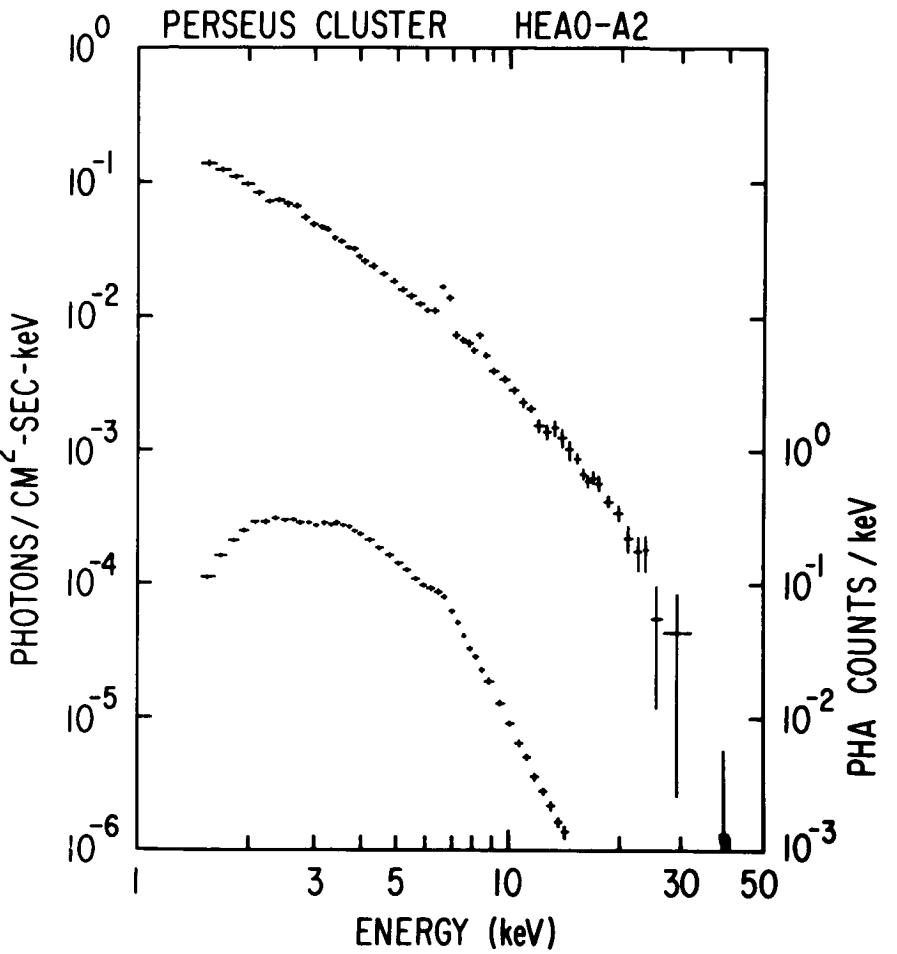

Figure 1. Data from an exposure to the Perseus cluster of galaxies taken with the Goddard HEAO-1 A2 proportional counter experiment. The lower points, for which the right-hand scale is appropriate, are the raw data in energy-equivalent pulse-height channels. The higher points, for which the left-hand scale is appropriate, represent the most probable input spectrum consistent with the assumption of an equilibrium thermal spectrum. Note, in particular, that the Kα and Kβ Fe emission lines at 6.7 keV and 7.9 keV can be enhanced for display by this model-dependent spectral inversion process.

manifestation of sufficient interactions between particles and photons that complete thermalization has occurred. X-ray "bursts" arising from nuclear burning episodes on the surfaces of neutron stars, for example, appear to exhibit these classic spectra.

The preponderance of X-ray sources typically exhibit intermediate continua in the sense that electron scattering plays a role in the formation of the observed spectra. This is true for the modified bremsstrahlung of the galactic binary systems which contain white dwarfs, neutron stars, or black holes, as well as for the active galactic nuclei which usually display a characteristic power law spectra with index $\alpha \sim 0.7$. Of particular relevance to this paper are the fluorescent line features which have been observed from both types.

Finally, the optically thin "thermal" spectra at "X-ray temperatures" of a variety of astrophysical system types provide the richest line spectra available to the next generation of instruments for X-ray spectroscopy. Optically thin plasmas offer a well studied starting point for comparison with actual X-ray source spectra. Although equilibrium and isothermality over the whole source volume may be a simpler situation than can be expected to obtain in general, less ideal sources can be modeled as a distribution of gases which exhibit thermal characteristics. The gas may be in local collisional equilibrium, so that the electrons will have local Maxwellian distributions with kinetic temperature T, while ions of charge Z may have the population fraction they would have in collisional equilibrium at a different temperature. The gas can have bulk motion, and parts of the source can be moving relative to one another. In complex sources, a nonthermal continuum may need to be taken into account, as well.

4. OPTICALLY THIN THERMAL SOURCES

In many astrophysical contexts, an X-ray-emitting plasma is sufficiently transparent that the emergent spectrum faithfully represents the microscopic processes occurring in the plasma. At temperatures $T > 10^8$ K, almost all abundant elements are fully ionized, and the X-ray emission is dominated by bremsstrahlung from hydrogen and helium. At lower temperatures,

however, trace elements retain a few atomic electrons, and their contribution to the emissivity of the plasma cannot be ignored. Because cross-sections for electron impact excitation of such ions far exceed those for bremsstrahlung or radiative recombination, line emission from $Z > 7$ constituents actually dominates the cooling from a plasma with $10^4 < T < 10^7$ K, even though these trace elements represent only $\sim 10^{-3}$ of the plasma composition by number.

A theoretical model is needed to infer physical parameters such as temperature, element composition, and density from the observed spectrum of an optically thin plasma. To construct such a model requires knowledge of the ionization state of each element, which is controlled by electron impact ionization and radiative and dielectronic recombination. If the plasma is maintained at constant temperature and density for a long time compared to the timescales for these microscopic processes, the ionization of trace elements relaxes to a stationary state that depends primarily on electron temperature and weakly on density. This stationary ionization balance assumption was first employed to interpret the solar corona, and many such "coronal models" have been calculated. An exemplary model spectrum is shown in Figure 2.

Such spectra are rich in emission lines and offer the opportunity to deduce many properties of the emitting gas when sufficient resolving power and sensitivity are available. The main emission complexes from Kα transitions of helium-like and hydrogenic ions of abundant elements such as O, Ne, Mg, Si, S, Ar, Ca, and Fe, become distinct with resolving power $R > 10$. A temperature may be inferred from the relative strengths of the helium-like and hydrogenic lines from a given element, but its validity depends on that of the stationary ionization balance assumption. A measure of temperature that is independent of that model assumption may be obtained from the ratio of Kβ to Kα transitions of a single ion if there is sufficient sensitivity to separate the weaker Kβ from Kα. With $R > 100$ a variety of more powerful temperature and density diagnostics become available. Satellite lines resulting from dielectronic recombination may be used as temperature diagnostics, and the Kα complexes of helium-like ions can be resolved into their resonance (2^1P), intercombination (2^3P), and forbidden (2^3S) components, where the relative strengths can be used to infer electron temperature and density.

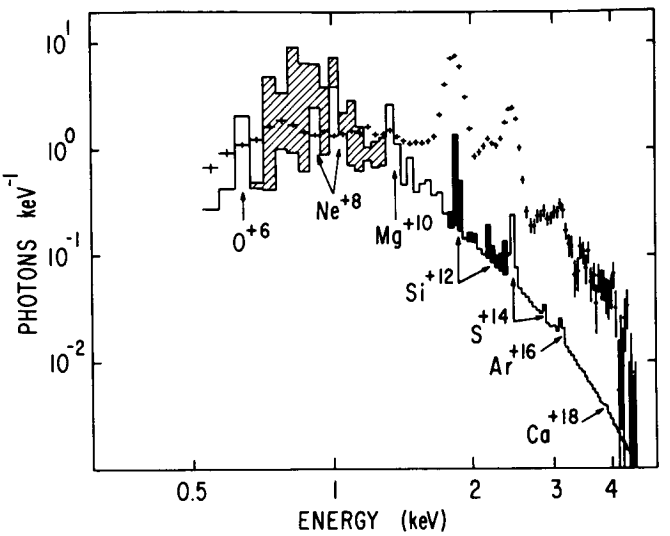

Figure 2. A comparison of the actual raw data from Tycho's SNR taken with the Goddard HEAO-2 solid-state spectrometer experiment and an idealized input spectrum. The data can be fit equally well with Sedov-blast-wave and two-temperature-equilibrium modeling, provided that the abundances of the even-Z elements are treated as free parameters. The idealized input spectrum represents the dominant $kT = 0.5$ keV component of the two-temperature fit to the data (the higher temperature component has $kT \sim 4$ keV), but with the abundances fixed at solar proportions. The shaded area represents the contribution from Fe L-blend emission at this temperature, and the blackened area represents the contribution form Si K-emission components. To facilitate comparison with the raw data (where the abscissa should properly be energy-equivalent pulse-height), the idealized input spectrum is viewed through a column density of 2×10^{21} atoms cm^{-2}. Both the data and the model are displayed in 46 eV bins, with the latter smeared to an effective resolution with FWHM ~ bin width (i.e. ~ 3 times better than the actual SSS FWHM resolution). The Kα and Kβ transitions of helium-like ions of Mg, Si, S, Ar, and Ca indicated on the model spectrum are clearly evident in the data. Since most of the K-emission arises from the lower temperature component of the two-temperature fit, it is clear that consistency with this model requires marked overabundances in the line-emitting species.

Without resolving power sufficient to determine a temperature distribution unambiguously, this distribution and the elemental abundances in the plasma must be non-uniquely determined from comparison with the data expected from a grid of models. For radiatively ionized or nonequilibrium plasmas, the model results are only as good as the reality of the model spectra. If a true equilibrium temperature distribution can be inferred, however, abundances can be determined by the comparison of lines of one element to those of other elements or to the continuum. Such abundance determinations are relatively straightforward for equilibrium plasmas, because each elemental constituent is present in just a few ionization states.

Information from less idealized situations can be gleaned with sufficient insight even when the optically thin equilibrium scenario is untenable. In the optically thin case, for example, inconsistency of the electron and ionization temperatures can be used to determine the extent to which the plasma is recombining or ionizing in a nonequilibrium situation. Colder material around or along the line of sight to the primary ionization can yield fluorescent lines, and optically thick plasmas can yield lines that are broadened by electron scattering. With sufficient resolving power, it may even be possible to measure the natural width of emission lines.

Many of the likely possibilities for X-ray spectra from astronomical objects, and the important information that the spectra might therefore reveal, can be found in reviews such as Holt and McCray [1982], from which much of the above introductory discussion has been taken.

5. REQUIRED RESOLVING POWER

A crucial consideration for any investigation is the sensitivity required to carry it out. For the X-ray spectroscopy of cosmic sources, a variety of parameters contribute to this sensitivity: the quantum efficiency of the detectors, the detector background, the detector bandpass, and the resolving power. If an "ideal" spectrometer with virtual unit efficiency, trivial background, and wide bandpass can be developed, then the only parameter which requires discussion is the resolving power.

Atomic physics prescribes the resolving power necessary to utilize various combinations of spectral lines for scientific study. For each element, we can approximate the resolving power required to separate a number of important ones. For n = (2 to 1) transitions, for example, the most important lines are those from the fluorescence of neutral material, the analog of Lyman α from hydrogen-like material, and the resonance, forbidden, and intercombination lines of helium-like material. The energy of Lyman α is, of course, Z^2 times the 10.2 eV for hydrogen. Table 1 gives the separation energies of these five lines for elements ($8 \leqslant Z \leqslant 26$) which are likely to be of interest for AXAF.

Table 1 demonstrates that while $\sim$ 1 eV may be required to completely resolve all the lines of potential interest from all elements, $\sim$ 10 eV is sufficient to separate the most important lines from oxygen, and can totally resolve them for iron.

TABLE 1: LINE SEPARATIONS

Line pairs	Approximate energy separation (eV)
Lyman α — Resonance	$10\ Z = 100\ Z_{10}$
Resonance — Intercombination	$0.32\ Z^{4/3} \sim Z$
Resonance — Forbidden	$0.77\ Z^{4/3} \sim 2\ Z$
Resonance — Neutral	$2.3\ \ Z^{3/2} \sim 10\ Z$

There is a similar $\sim$ 10 eV requirement commensurate with possible sources of line broadening. The natural width of a resonance line is $\sim 10^{-2} Z_{10}^{\ 4}$ eV, so that resonance and even narrower forbidden lines have widths that are not measurable with $\sim$ 1 eV. Thermal broadening at $\sim 2(T_8 Z_{10}^{\ 3})^{1/2}$ eV would similarly require sub-eV resolution to measure, even for the heaviest elements at the highest temperatures. Broadening associated with mass motion is easily discernible in many astrophysical contexts with 10 eV, however, as the broadening for this case is $\sim 4 v_{1000} Z_{10}^{\ 2}$eV ($v_{1000}$ in units of 1000 km s^{-1}).

It would appear, therefore, that the few-eV resolution required for the study of all the diagnostics in Table 1 is well matched to that required for the motion-broadening in active galactic nuclei (AGN), young supernova remnants (SNR), and the strong stellar winds of early type stars. The resolving power required to measure thermal or natural broadening would be orders of magnitude better, however.

6. AN "IDEAL" SPECTROMETER

The most important attributes of a spectrometer depend upon the specific scientific objectives of a particular investigation, but there are some which are so generally useful that they can be safely assumed to be characteristic of the "ideal" spectrometer for AXAF. These attributes include energy resolution sufficient to address the most important scientific objectives for all classes of sources and sensitivity to the entire AXAF bandpass simultaneously with both near-unit efficiency and trivial background.

The X-ray calorimeter (see Figure 3) which has been selected as part of the AXAF study payload promises these attributes. It consists of an X-ray absorber of heat capacity C loosely connected to a heat sink of temperature T by a thermal link with conductivity G. When a photon of energy Q is absorbed, it is degraded into quanta (phonons) characteristic of T. The temperature of the absorber rises by an amount $\delta T = Q/C$ and then decays back to its equilibrium temperature with a time constant $\tau = C/G$. The temperature increase is detected by a thermistor attached to the absorber, and the incoming photon energy can be deduced by the magnitude of δT.

The small heat deposition is measurable to a precision which is determined by the random exchange of energy between the detector and its heat bath through the thermal link. An oversimplified "explanation" of the situation is that the effective number of phonon modes contributing to the heat capacity and to the fluctuations is $N = C/k$, each with effective mean energy kT. If the typical quantum occupation number in each mode is unity, the rms fluctuation in that number is also unity. Therefore, the total energy fluctuation in the system is $\delta E \sim kT(N^{1/2}) \sim (kT^2C)^{1/2}$.

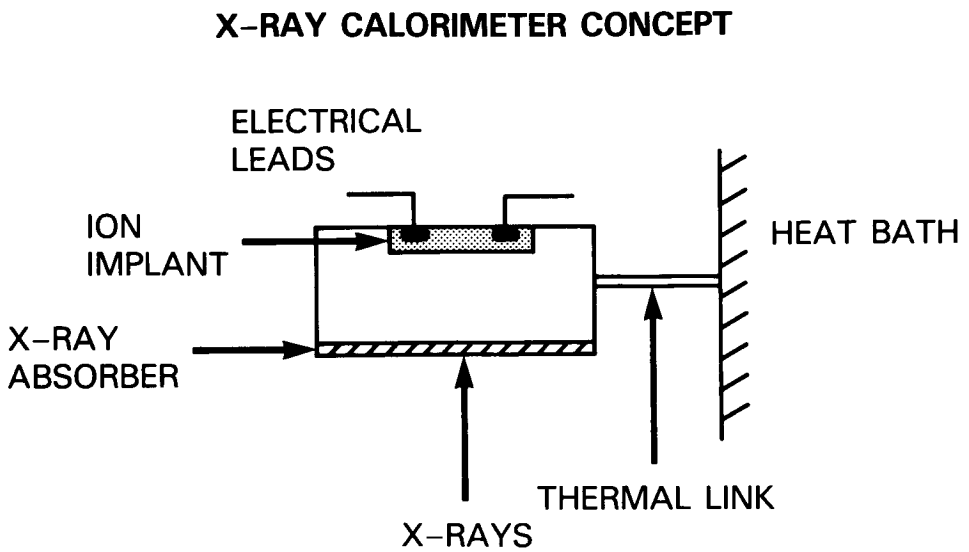

Figure 3. Schematic of an X-ray calorimeter. The essential elements are an X-ray absorber, a temperature transducer, and a thermal link to a heat bath which is loose enough to ensure that the rise in temperature accurately reflects the deposited energy (i.e., that the timescale for total thermalization of the X-ray energy is short compared with the characteristic time constant of the thermal link).

Because the number of phonons involved in the final steps of degradation of phonon energy to heat is large, the statistical fluctuations which fundamentally limit the resolution of charge collecting detectors (such as Si(Li) or proportional counters) do not significantly affect the temperature increase produced by a single photon; this means that the limiting FWHM resolution of the device will be uniform over the whole bandpass.

When all necessary noise contributions (such as load resistor Johnson noise and realistic filter techniques) are taken into account, the limiting resolution of a practical detector is δE (FWHM) $\sim 4(kT^2C)^{1/2}$ [Moseley, Mather, and McCammon, 1984], which can be as low as 1 eV for a detector with total heat capacity $< 10^{-14}$ J/K operating at 0.1 K. Such detectors can be designed

for AXAF, but it remains to demonstrate that the theoretically predicted performance can actually be obtained.

7. RECENT PROGRESS IN DETECTOR DEVELOPMENT

There are two general types of noise source which can potentially prevent the achievement of the theoretical performance discussed above. The first might be called "conversion" noise, as it arises from the imperfect conversion of X-ray energy to phonons, e.g., energy which goes into electric charge or which is trapped in states with long lifetimes. The second might be called "readout" noise, as it arises from imperfect transduction of the temperature increase into interpretation as an energy deposition.

The latter potential noise source may be ultimately limiting in attempting to attain 1 eV, but it has already been experimentally demonstrated to be < 10 eV via the observation of fluctuations in the sampling of the baseline of a test detector with heat capacity higher than the value required for 1 eV [Moseley et al., 1985]. Since we could not simultaneously demonstrate similarly low conversion noise, our efforts during the past year have been aimed at understanding and reducing this component. We have recently succeeded in achieving that level of conversion noise via the comparison of X-ray resolution with conversion-independent baseline fluctuations.

Figure 4 demonstrates the performance of a nonoptimized composite detector with baseline fluctuations of $\sim$ 30 eV FWHM. An overnight run was performed with an Fe^{55} source, yielding a total additional noise contribution (including conversion noise) of < 10 eV in the K-capture lines and in fluorescence from an Mg target. It is interesting to note that the Kα line is better modeled with its two components (Kα1 and Kα2) than with a single line, and that their separation of $\sim$ 10 eV is at about the current level at which we can demonstrate the contribution from either conversion or readout sources (although the latter contribution in this particular detector is three times larger).

There still remain subtle problems with the production of 1 eV detectors, but we have now demonstrated that 10 eV detectors can be made. Our goal is

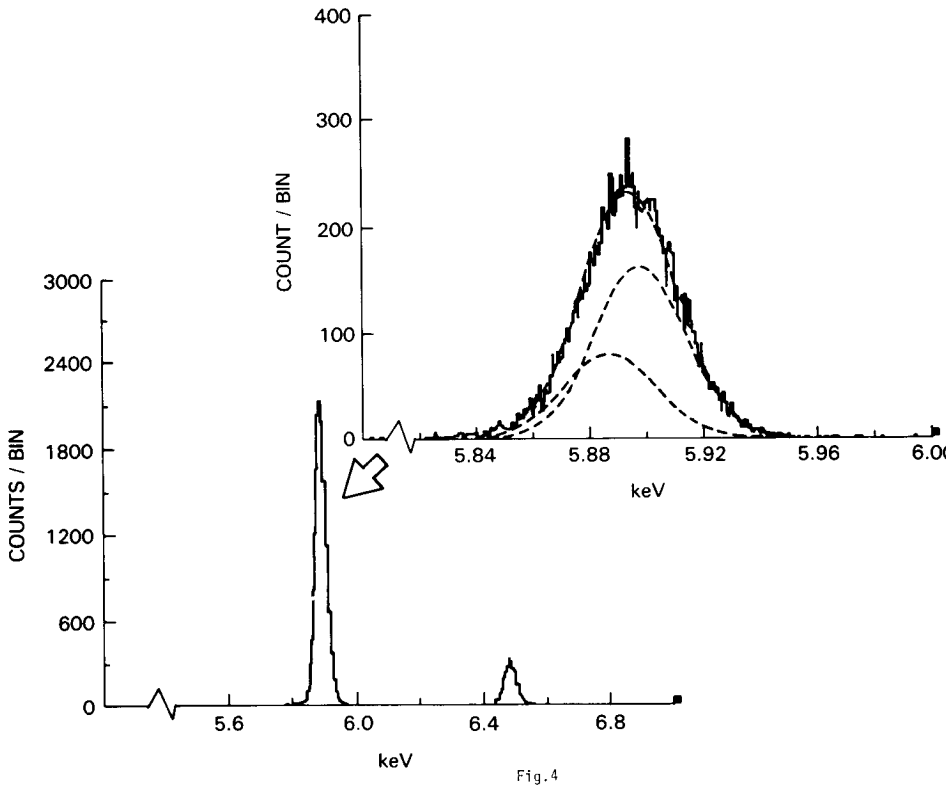

Figure 4. Raw data from an Fe^{55} X-ray source taken with a composite calorimeter consisting of a HgCdTe X-ray absorber on a Si substrate with an ion-implanted thermistor. The Kβ line is ~ 600 eV higher in energy than Kα, and an order of magnitude less prominent. The Kα line has two major components separated by ~ 10 eV, with the higher energy component approximately twice as prominent. These two Kα components are required for an acceptable fit to the data, but cannot be resolved by the current ~ 30 eV detector. The AXAF detector should be capable of completely resolving them.

to produce detectors for AXAF for which Kα1 and Kα2 from Fe^{55} will be completely resolved. Note that the spatial resolution of the AXAF telescope (< 1 arc-sec ~ 0.05 mm) is required in order to reach this goal, as the necessary value of C cannot be attained without a sub-mm sized detector.

8. SUMMARY

The AXAF microcalorimeter provides a totally new capability for X-ray astronomical spectroscopy. The combination of resolving power of order 10^3 with quantum efficiency of order unity (with virtually insignificant detector background) simultaneously over the entire AXAF bandpass allows for the application of X-ray spectroscopy to much more ambitious scientific studies than previously possible.

The X-ray astronomy group at Goddard has made numerous contributions to astrophysics, and no subject represents its experimental motivation more than does X-ray spectroscopy. It is particularly fitting for the purposes of this volume that the microcalorimeter, the latest manifestation of this experimental research program, has arisen out of a true collaboration between the Goddard X-ray and infrared groups, both of which owe their existence to the foresight of Frank McDonald.

REFERENCES

Giacconi, R., Gursky, H., Paolini, F., and Rossi, B., 1962, *Phys. Rev. Letters.*, **9**, 439.

Giacconi, R. et al., 1979, *Astrophys. J.*, **230**, 540.

Holt, S. S., Boldt, E. A., and Serlemitsos, P. J., 1969, *Astrophys. J.*, **153**, L137.

Holt, S. S., and McCray, R., 1982, *Ann. Rev. Astron. Ap.*, **20**, 323.

Moseley, S. H., Kelley, R. L., Mather, J., Mushotzky, R. F., Szymkowiak, A. E., and McCammon, D., 1985, *IEEE Trans. Nucl. Sci.*, **NS-32**, 134.

Moseley, S. H., Mather, J., and McCammon, D., 1984, *J. Appl. Phys.*, **56**, 1263.

Schreier, E., Levinson, R., Gursky, H., Kellogg, E., Tananbaum, H., and Giacconi, R., 1972, *Astrophys. J.*, **172**, L79.

Serlemitsos, P. J., Boldt, E. A., Holt, S. S., Ramaty, R., and Brisken, A. F., 1973, *Astrophys. J.*, **184**, L1.

Serlemitsos, P. J., Boldt, E. A., Holt, S. S., Rothschild, R. E., Saba, J. L. R., 1975, *Astrophys. J.*, **201**, L9.

Van der Klis, M., et al., 1985, *Nature*, **316**, 225.

Weisskopf, M. C., Silver, E. H., Kestenbaum, H. L., Long, K. S., and Novick, R., 1978, *Astrophys. J.*, **220**, L117.